THE JOURNAL OF BIOLOGICAL CHEMISTRY VOL. 284, NO. 42, pp. 29180–29192, October 16, 2009

Through the Looking Glass, Mechanistic Insights from Enantiomeric Human Defensins*[S]

Received for publication, May 11, 2009, and in revised form, July 14, 2009 Published, JBC Papers in Press, July 29, 2009, DOI 10.1074/jbc.M109.018085

Gang Wei[‡§1,2], Erik de Leeuw[‡1], Marzena Pazgier[‡1], Weirong Yuan[‡], Guozhang Zou[‡], Jianfeng Wang[‡], Bryan Ericksen[‡], Wei-Yue Lu[§], Robert I. Lehrer[¶], and Wuyuan Lu[‡3]

From the [‡]Institute of Human Virology, University of Maryland School of Medicine, Baltimore, Maryland 21201, the [§]School of Pharmacy, Fudan University, Shanghai 201203, China, and the [¶]Department of Medicine, David Geffen School of Medicine, UCLA, Los Angeles, California 90095

Despite the small size and conserved tertiary structure of defensins, little is known at a molecular level about the basis of their functional versatility. For insight into the mechanism(s) of defensin function, we prepared enantiomeric pairs of four human defensins, HNP1, HNP4, HD5, and HBD2, and studied their killing of bacteria, inhibition of anthrax lethal factor, and binding to HIV-1 gp120. Unstructured HNP1, HD5, and HBD3 and several other human α- and β-defensins were also examined. Crystallographic analysis showed a plane of symmetry that related ^{L}HNP1 and ^{D}HNP1 to each other. Either D-enantiomerization or linearization significantly impaired the ability of HNP1 and HD5 to kill *Staphylococcus aureus* but not *Escherichia coli*. In contrast, ^{L}HNP4 and ^{D}HNP4 were equally bactericidal against both bacteria. D-Enantiomers were generally weaker inhibitors or binders of lethal factor and gp120 than their respective native, all-L forms, although activity differences were modest, particularly for HNP4. A strong correlation existed among these different functions. Our data indicate: (*a*) that HNP1 and HD5 kill *E. coli* by a process that is mechanistically distinct from their actions that kill *S. aureus* and (*b*) that chiral molecular recognition is not a stringent prerequisite for other functions of these defensins, including their ability to inhibit lethal factor and bind gp120 of HIV-1.

Defensins are 2–5 kDa, disulfide-stabilized cationic peptides found in the leukocytes and epithelial tissues of mammals (1–5). On the basis of disulfide topology, defensins are classified into three structural families: α, β, and θ. To date, six human α-defensin peptides, also known as human neutrophil peptides (HNPs)[4] 1–4 and enteric defensins 5–6 (HD5 and HD6) have been identified. Many more human β-defensins (HBDs) exist and are believed to be expressed predominantly in epithelia. However, only a few of these have been characterized thus far at the protein level (6). Macrocyclic θ-defensins are expressed in the leukocytes and bone marrow of certain nonhuman primates, but not of humans (7). Despite differences in amino acid composition, Cys connectivity and tissue distribution, mammalian α- and β-defensins are structurally conserved, adopting a three-stranded β-sheet core structure stabilized by three intramolecular disulfide bonds. At the functional level, however, defensins exert extremely diverse effects.

Originally identified as "natural peptide antibiotics" (8, 9), defensins act early in innate immune defenses against potentially infectious bacteria, fungi, and viruses. It is generally accepted that bacterial killing by defensins is initiated by a "fatal attraction" between the cationic defensins and the anionic microbial membrane that culminates in target cell death elicited by microbial membrane disruption and leakage of cellular contents (10, 11). An array of molecular mechanisms has been suggested to account for the ability of defensins to inhibit both enveloped and non-enveloped viruses. For HIV-1 alone, at least six distinct modes of action have been proposed, including direct inactivation of virions (12–15), interference with protein kinase C signaling and viral replication (12), up-regulation of CC-chemokines (16), inhibition of gp41-membrane fusion (17), inhibition of CD4-gp120 interactions (18), and down-regulation of HIV co-receptors (14). Adding to this complexity is a recent finding that HD5 and HD6 enhance HIV-1 infection during viral entry, acting via some unknown mechanism (19).

Defensins also appear to be important immunomodulators, capable of acting on a variety of cellular receptors and host proteins (3, 20, 21). For example, defensins chemoattract and activate different types of immune cells (22–25), regulate cytokine production (26, 27), interact with components of the complement system (28, 29), and participate in wound healing by promoting epithelial cell migration and proliferation (30, 31). More recently, β-defensins have been shown to bind with high affinity to melanocortin receptors to signal pigment-type switching in dogs (32).

Defensins also neutralize many secreted bacterial toxins (33), including anthrax lethal toxin (LeTx), a binary complex of two bacterial proteins secreted by *Bacillus anthracis*, protective antigen and lethal factor (LF) (34, 35). LF is a Zn^{2+}-dependent metalloprotease, which, upon entering macrophages, cleaves important cellular proteins, induces cell death, and is the pri-

* This work was supported, in whole or in part, by National Institutes of Health Grants AI072732 and AI061482 (to W. L.).

The atomic coordinates and structure factors (codes 3gny and 3go0) have been deposited in the Protein Data Bank, Research Collaboratory for Structural Bioinformatics, Rutgers University, New Brunswick, NJ (http://www.rcsb.org/).

[S] The on-line version of this article (available at http://www.jbc.org) contains supplemental Table S1 and Figs. S1 and S2.

[1] These authors contributed equally to this work.

[2] Supported by the National Natural Science Foundation of China (Grant 30701060).

[3] To whom correspondence should be addressed: Tel.: 410-706-4980; Fax: 410-706-7583; E-mail: wlu@ihv.umaryland.edu.

[4] The abbreviations used are: HNP, human neutrophil peptide; HBD, human β-defensin; HIV-1, human immunodeficiency virus, type 1; RU, response units; TSB, tryptic soy broth; LeTx, lethal toxin; LF, lethal factor; SPR, surface plasmon resonance.

mary virulence factor in the pathogenesis of anthrax. Kaufmann and colleagues first reported that HNP1–3 non-competitively inhibited LF and protected cells as well as experimental animals against killing induced by *B. anthracis* LeTx (36). *B. anthracis* spores engulfed by human neutrophils germinated intracellularly, only to then be killed effectively by HNPs (37). Inhibition of LF and killing of vegetative cells of *B. anthracis* by retrocyclins, putative hominid homologues of rhesus monkey θ-defensins encoded by human pseudogenes, have also been reported (38).

Aside from their ability to interact with bacterial membranes and a variety of proteins, many defensins also bind carbohydrates, nucleic acids, and lipids. Retrocyclins, for example, inhibit influenza virus infection by cross-linking glycoproteins on the (host) membrane surface, thus preventing hemagglutinin-mediated viral fusion and entry (39). Some antiviral activities of defensins appear to be associated with their lectin properties (40–42). How such small peptides have acquired functional versatility or promiscuity at the molecular level remains obscure. To better understand defensin functionality in innate and adaptive immunity, we compared HNP1, HNP4, HD5, and HBD2 with their enantiomeric counterparts, made up entirely of D-amino acids, with respect to bacterial killing, LF inhibition, and HIV-1 gp120 binding. High resolution crystal structures of the enantiomeric pair of HNP1 were determined. Hoping to gain additional mechanistic insights, we examined five other human defensins (HNP2, HNP3, HD6, HBD1, and HBD3), as well as linearized analogs of HNP1, HD5, and HBD3 whose six Cys residues were all replaced by either Ala or α-aminobutyric acid.

EXPERIMENTAL PROCEDURES

Materials—Synthesis of HNP1–4, HD5–6, and HBD1–3 was done as described previously (43–45). The D-enantiomeric defensins ^{D}HNP1, ^{D}HNP4, ^{D}HD5, and ^{D}HBD2 were prepared similarly to their natural counterparts using D-amino acids and custom-made 4-hydroxymethylphenylacetamidomethyl resins. The three unstructured/linearized defensin analogs, Ala-HNP1, α-aminobutyric acid-HD5, and α-aminobutyric acid-HBD3, were synthesized on an ABI 433A peptide synthesizer using the published 2-(1H-benzotriazolyl)-1,1,3,3-tetramethyluroniumhexafluorophosphate activation/*N*,*N*-diisopropylethylamine *in situ* neutralization protocol for *t*-butoxycarbonyl chemistry (46). All peptides were purified to homogeneity by C18 reversed-phase high-performance liquid chromatography, and their molecular masses were verified by electrospray ionization mass spectrometry. Quantification of defensins was done by UV measurements at 280 nm using molar extinction coefficients calculated from a published algorithm (47).

Recombinant anthrax lethal factor and protective antigen were purchased from List Biological Laboratories, Inc. A sequence-optimized chromogenic substrate of lethal factor, Ac-NleKKKKVLP-*p*-nitroaniline, was synthesized essentially as described (48). In brief, a peptide acid precursor, Ac-NleKKKKVL-OH, whose lysine side chains were orthogonally protected by *t*-butoxycarbonyl, was first synthesized on 2-chlorotrityl chloride resin using a standard Fmoc (*N*-(9-fluorenyl)methoxycarbonyl) chemistry and cleaved in a mixture of acetic acid/trifluoroethanol/dichloromethane (1:2:7). Coupling of Pro-*p*-nitroaniline to the C terminus of the precursor peptide was achieved using 2-(1*H*-benzotriazolyl)-1,1,3,3-tetramethyluroniumhexafluorophosphate and *N*,*N*-diisopropylethylamine in dimethylformamide for 2 h. The product was precipitated and washed by ice water, deprotected by trifluoroacetic acid, and purified to homogeneity by reversed-phase high-performance liquid chromatography. HIV_{BaL} gp120, expressed in T-REx^{TM}-293 cells and affinity-purified, was a generous gift from Profectus Biosciences, Inc.

LF Inhibition Kinetics—The inhibition of LF by various defensins was quantified using an enzymatic kinetic assay (36, 48). Briefly, freshly prepared LF at a final concentration of 1 μg/ml (~10 nM) was incubated at 37 °C for 30 min with a 2-fold dilution series of defensin in 20 mM HEPES buffer containing 1 mM $CaCl_2$ and 0.5% Nonidet P-40, pH 7.2. 20 μl of LF substrate (1 mM in the buffer) was added to each well to a final concentration of 100 μM in a total volume of 200 μl. The enzyme activity, characterized as a time-dependent absorbance increase at 405 nm due to the release of *p*-nitroaniline, was monitored at 37 °C over a period of 5 min on a 96-well V_{max} microplate reader (Molecular Dynamics, Inc.). Data are presented in a plot showing percent inhibition *versus* defensin concentration, from which IC_{50} values (the concentration of defensin that reduced the enzymatic activity of LF by 50%) were derived by a non-linear regression analysis.

Surface Plasmon Resonance-based LF and gp120 Binding—Experiments were performed on a BIAcore T100 System (BIAcore, Inc., Piscataway, NJ), unless stated otherwise, at 25 °C in 10 mM HEPES, 150 mM NaCl, 0.05% surfactant P20, pH 7.4 (±3 mM EDTA). LF was immobilized on a CM5 sensor chip at a level of 2500 response units (RU) by the amine-coupling protocol. HIV gp120 chips were prepared at 2830 and 3200 RU. Analytes were introduced into the flow-cells at 30 μl/min in the running buffer. Association and dissociation were assessed for 5 and 10 min, respectively. Resonance signals were corrected for non-specific binding by subtracting the background of the control flow-cell. After each analysis, the sensor chip surfaces were regenerated with 10 mM glycine solution (pH 2.0) and 50 mM NaOH for LF or 10 mM NaOH for gp120 and equilibrated with the buffer before next injection. Binding isotherms were analyzed with BIAevaluation software and/or GraphPad Prism.

Virtual Colony Count—Antimicrobial assays against *Escherichia coli* ATCC 25922 and *Staphylococcus aureus* ATCC 29213 (Microbiologics) were conducted using a previously detailed 96-well turbidimetric method dubbed "virtual colony counting" (49). A 2-fold dilution series of defensin, ranging from 256 to 1 μg/ml in 10 mM sodium phosphate, pH 7.4, was incubated at 37 °C for 2 h with *E. coli* or *S. aureus* (1×10^6 CFU/ml), followed by addition of twice-concentrated Mueller-Hinton broth (2×) and kinetic measurements of bacterial growth at 650 nm over 12 h. To increase the sensitivity of bacterial killing by some defensins, 1% tryptic soy broth (TSB) was added to the phosphate buffer during the 2-h incubation period. The virtual LD_{50} (vLD_{50}), vLD_{90}, vLD_{99}, and $vLD_{99.9}$ were reported as the defensin concentration that resulted in survival rates of 0.5, 0.1, 0.01, and 0.001, respectively.

Crystallization and Data Collection—Crystallization screenings were conducted at room temperature using the hanging-drop, vapor diffusion method and the commercially available crystallization Sparse Matrix Screens (Hampton Research). The drops were generated by mixing 0.5 μl of defensin solution (prepared at 20 mg/ml in water) with 0.5 μl of reservoir solution, and placed over 0.8 ml of reservoir solution. HNP1 crystals were grown from mother liquor containing 0.1 M imidazole and 1.0 M sodium acetate trihydrate, pH 6.5, whereas ^{D}HNP1 crystals from 0.1 M sodium citrate tribasic dehydrate, 0.1 M HEPES sodium, and 20% (v/v) isopropanol, pH 7.5. In both cases the crystals appeared after 1 day and grew to the final sizes within a week.

Prior to freezing in a 100 K stream of nitrogen, crystals were briefly soaked in crystallization solutions with 20% glycerol (w/v) added. X-ray diffraction data were collected from flash-frozen crystals mounted on a rotating anode x-ray generator Rigaku-MSC Micromax 7 equipped with a Raxis-4++ image plate detector (at the x-ray Crystallography Core Facility, University of Maryland, Baltimore). Crystal diffraction images were indexed, integrated, scaled and merged using the HKL2000 package (50). Both defensins crystallized in the orthorhombic form and belong to the space group $P2_12_12$. The data collection statistics are shown in supplemental Table S1.

Structure Determination and Refinement—The structure of HNP1 was solved by molecular replacement using the program Phaser from the CCP4 suite (51) with the HNP3 molecule (1DFN (52)) as a search model. The refined structure of HNP1 was subsequently used as an initial model for ^{D}HNP1 structure determination with Phaser. The structures were refined to 1.56 Å with the program Refmac (53), and the models were corrected by manually re-fitting into the electron density and rebuilt using the program COOT (54). The results of refinement are summarized in supplemental Table S1. The coordinates and structure factors have been deposited in the Protein Data Bank with accession codes of 3gny and 3go0 for HNP1 and ^{D}HNP1, respectively. Molecular graphics were generated using PyMOL (DeLano Scientific LLC, San Carlos, CA).

RESULTS

Structural Studies—Ideally, an unnatural protein that is composed entirely of D-amino acids is the mirror image of its native form comprising only L-amino acids in the same sequence. Two mirror image proteins (enantiomers), in identical amounts, rotate the plane of polarized light equally, but in opposite directions. When the paired defensin enantiomers, ^{L}HNP1/^{D}HNP1, ^{L}HNP4/^{D}HNP4, ^{L}HD5/^{D}HD5, and ^{L}HBD2/^{D}HBD2, were examined by CD spectroscopy, the spectra of each enantiomeric defensin pair appeared symmetrical about the *x*-axis (supplemental Fig. S1), characteristic of two optically active chiral molecules related to one another by a plane of symmetry. ^{L}HNP1 and ^{D}HNP1 were chosen for further characterization by x-ray crystallography. Both defensins crystallized rapidly in the orthorhombic system and diffracted to 1.56 Å on our home x-ray source with the final values of R (R_{free}) of 0.171 (0.185) and 0.191 (0.199), respectively (supplemental Table S1). The crystal structures of ^{L}HNP1 and ^{D}HNP1, with two defensin molecules present in one asymmetric unit, are shown in Fig. 1*A*. As expected, ^{L}HNP1 adopts the canonical three-stranded β-sheet fold arranged in a dimeric form, which is conserved in the α-defensin family (55), whereas ^{D}HNP1 shows a nearly perfect mirror image of its native L-counterpart. The vast majority of the side-chain conformations, with a few exceptions, are also preserved symmetrically between ^{L}HNP1 and ^{D}HNP1. When the dimers (60 residues) of ^{L}HNP1 and an inverted ^{D}HNP1 were superimposed, the root mean square deviations were found to be 0.17 Å for C_α atoms and 0.5 Å for all atoms (Fig. 1*B*). In addition to the flexible termini, the loop region connecting the second and third β strands of monomer B (residues Gln-22 and Gly-23) constitutes a notable local structural difference between ^{L}HNP1 and ^{D}HNP1, characterized by a larger than normal root mean square deviation. Because the β2–β3 loop of ^{D}HNP1 is involved in substantial crystal contacts, the observed difference likely resulted from the effect of crystal packing rather than intrinsic properties of the backbone.

Synthetic HNP1 Neutralizes LeTx—For validation purposes, we characterized the ability of our synthetic HNP1 to neutralize cytotoxicity of anthrax LeTx in murine macrophages (supplemental Fig. S2). We measured *in vitro* protective activity of HNP1 against LeTx (400 ng/ml LF and 1600 ng/ml protective antigen) using the same assay protocols as described by Kim *et al.* (36). Shown in supplemental Fig. S2 is HNP1 dose-dependent protection of RAW 264.7 cells against cytolysis by LeTx assayed in RPMI medium 1640 supplemented with 5% fetal calf serum. Three independent experiments were performed, giving rise to a highly reproducible EC_{50} value of 15 ± 1 μM (effective concentration of HNP1 at which 50% cell viability is observed), in quantitative agreement with the value reported by Kim *et al.* (36). Consistent with these findings, a Trypan blue cell staining experiment showed that 20 μM synthetic ^{L}HNP1 fully protected murine macrophages from LeTx-induced cytolysis with no apparent cytotoxicity.

D-Defensins Are Weaker Inhibitors of LF Than L-Defensins—LF inhibition by a 2-fold, 11-point dilution series of ^{L}HNP1 (0, 1, 2, 4, 8, 16, 32, 64, 128, 256, 512, and 1024 nM) was quantified at 37 °C using an enzyme kinetic assay protocol tailored from the published procedures developed by Kaufmann and colleagues (36). Shown in Fig. 2*A* is a percent residual LF activity plot *versus* defensin concentration on a log scale, obtained from 24 independent measurements. Complete inhibition of 10 nM LF was achieved by HNP1 at ≥1024 nM. A non-linear regression analysis yielded an IC_{50} value of 148 ± 11 nM, similar to the IC_{50} value of 190 ± 33 nM reported by Kim *et al.* (36). We also quantified LF inhibition by ^{D}HNP1, ^{L}HNP4/^{D}HNP4, ^{L}HD5/^{D}HD5, and ^{L}HBD2/^{D}HBD2 (Fig. 2*A*). On the basis of their IC_{50} values, the four L-defensins ranked in the following order of activity: ^{L}HNP1 (148 nM) ≈ ^{L}HD5 (194 nM) > ^{L}HNP4 (811 nM) ≫ ^{L}HBD2 (22.9 μM). ^{L}HBD2 was substantially weaker than the three $^{L}\alpha$-defensins. The inhibition curve of HNP4 was relatively steep, with percent residual LF activity dropping from ~90% to almost zero as the defensin concentration increased from 516 to 2048 nM. By contrast, ^{L}HD5, despite a significantly lower IC_{50} value, did not cause complete LF inhibition even at 2048 nM. Notably, the order of activity of D-defensins remained roughly the same, *i.e.* ^{D}HNP1 (961 nM) ≈ ^{D}HD5 (700 nM) > ^{D}HNP4 (1.59 μM) ≫ ^{D}HBD2 (72.6 μM). Enantiomerization

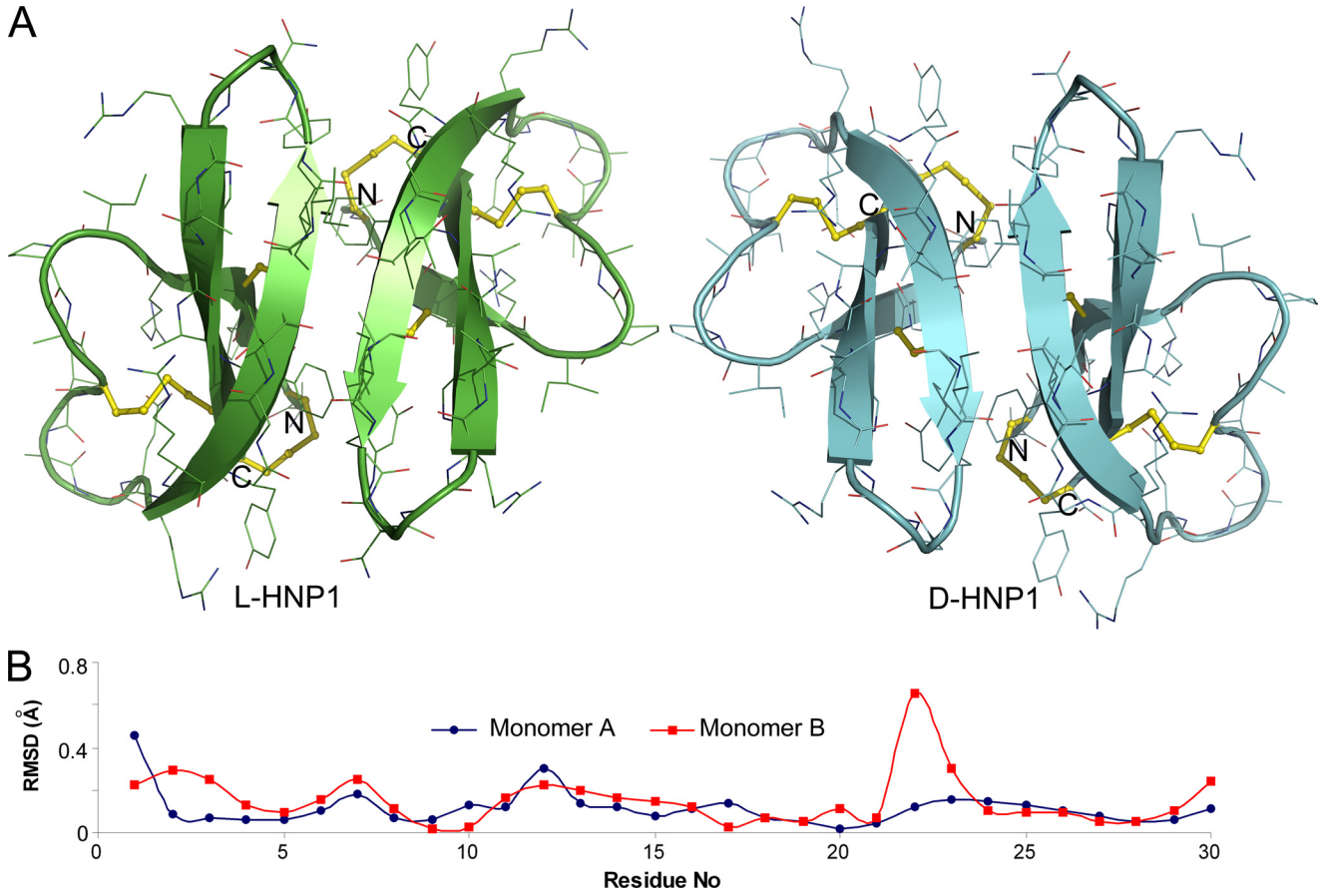

FIGURE 1. **Crystal structures of ^{L}HNP1 and ^{D}HNP1 related to one another by a plane of symmetry.** *A*, *ribbon diagrams* of HNP1 dimers in the asymmetric unit of ^{L}HNP1 and ^{D}HNP1 crystals. The three conserved disulfide bridges are shown as *yellow sticks*. *B*, root mean square deviations of C_α atoms between two enantiomeric monomers of HNP1. Monomers A and B of ^{L}HNP1 were compared with monomers A and B of inverted ^{D}HNP1, respectively.

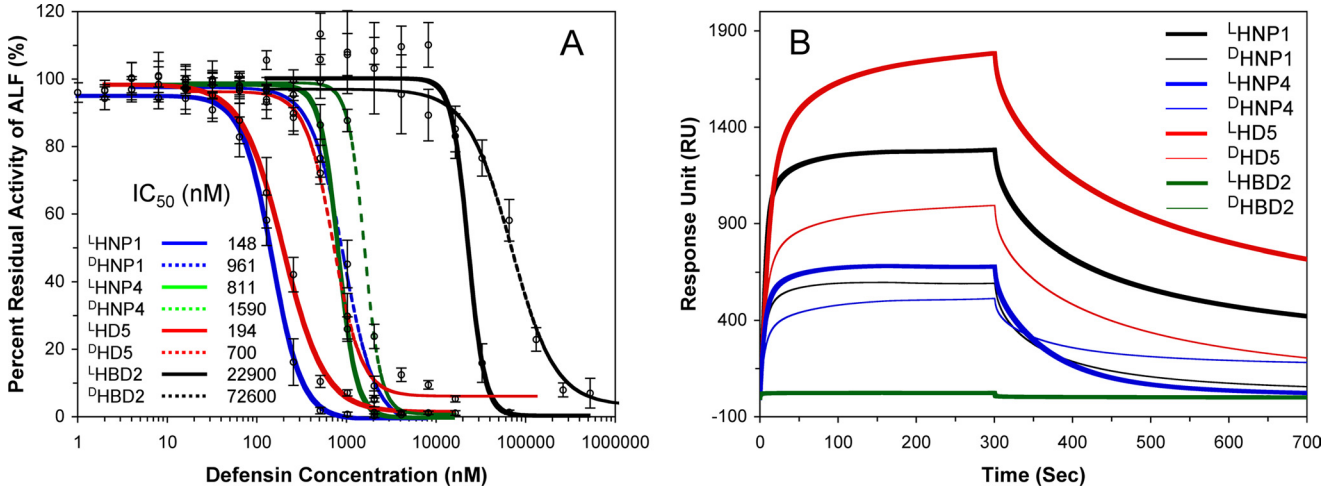

FIGURE 2. **Inhibition and binding of LF by enantiomeric defensins.** *A*, inhibition of LF activity by different concentrations of L- (*solid line*) or D-defensin (*dotted line*). The data are averages of three independent enzyme kinetic measurements, except for ^{L}HNP1, for which 24 independent measurements were performed. A Student *t*-test was used to calculate the *p* values for statistical significance: $p = 0.0084$ for ^{L}HNP1/^{D}HNP1; $p = 0.066$ for ^{L}HNP4/^{D}HNP4; $p = 0.014$ for ^{L}HD5/^{D}HD5; and $p = 0.17$ for ^{L}HBD2/^{D}HBD2. *B*, representative sensorgrams of L (*thick lines*)- and D (*thin lines*)-defensins, each at 1 μM, on 2500 RU of immobilized LF.

impacted defensin activity differentially, as evidenced by an almost 7-fold increase in IC_{50} of ^{D}HNP1, a more modest 3- to 4-fold increase in IC_{50} of ^{D}HD5 or ^{D}HBD2, and a merely 2-fold increase in IC_{50} of ^{D}HNP4.

Using SPR, we compared LF binding kinetics of L- and D-defensins at various peptide concentrations (62.5, 125, 250, and 500 nM and 1 and 2 μM for HNP1 and HD5; 62.5, 125, 250, and 500 nM and 1, 2, and 4 μM for HNP4; and 0.5, 1, 2, 4, 8, 16, and 32 μM for HBD2). Representative sensorgrams of the eight defensins at 1 μM each on 2500 RU of LF are shown in Fig. 2*B*. Unlike the enantiomeric β-defensins ^{L}HBD2 and ^{D}HBD2, the six α-defensins, and ^{L}HNP1 and ^{L}HD5 in particular, bound

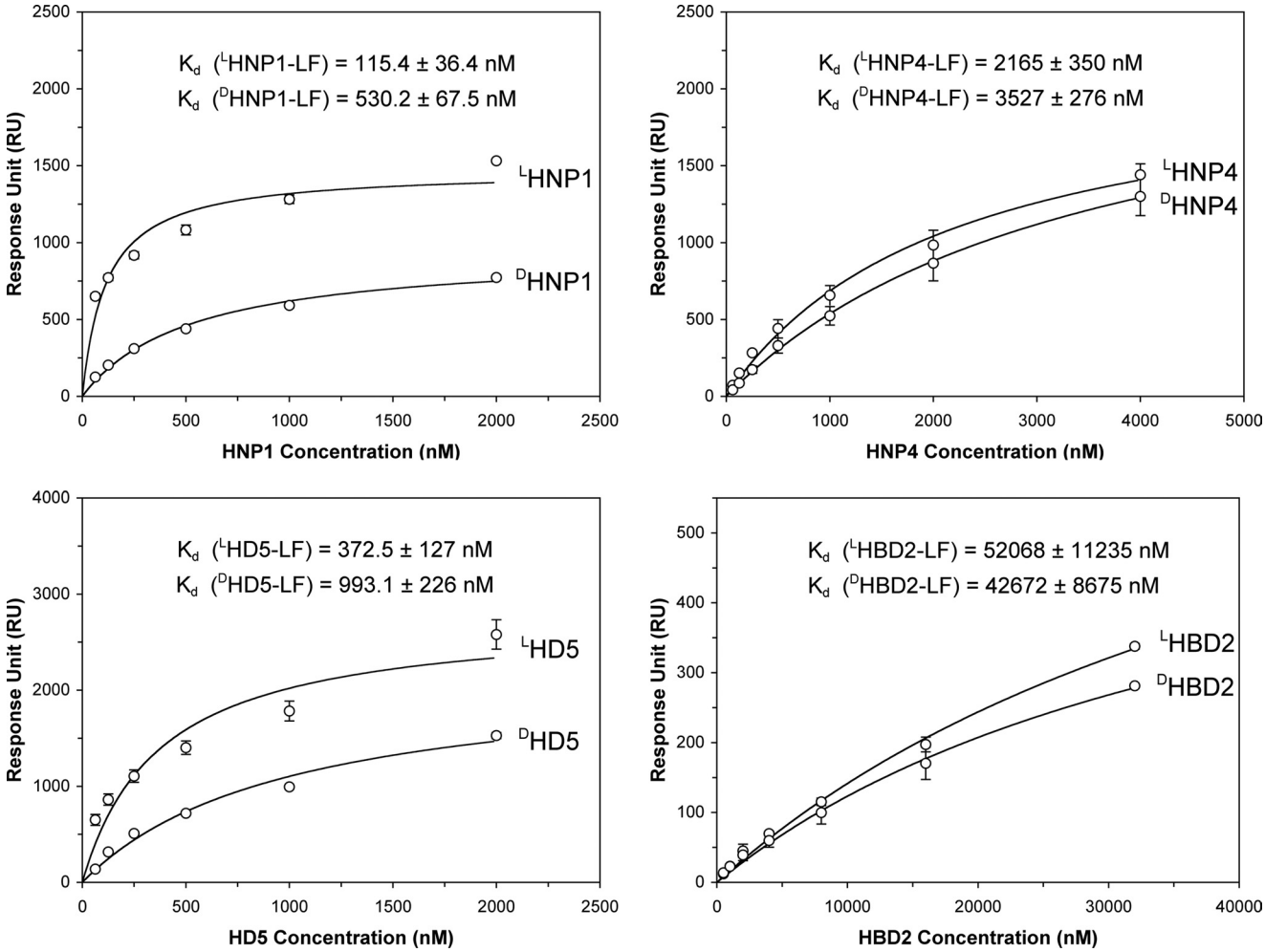

FIGURE 3. **Enantiomeric defensins bound to 2500 RUs of immobilized LF as a function of concentration.** The RU values collected at t = 300 s from three independent SPR measurements were fitted to a one-site binding model ($Y = B_{max} \cdot X/[K_d + X]$) using Graphpad Prism version 4.0. The *p* values were calculated using a Student's t-Test: $p < 0.001$ for ^{L}HNP1/^{D}HNP1; $p = 0.0019$ for ^{L}HNP4/^{D}HNP4; $p < 0.001$ for ^{L}HD5/^{D}HD5; $p = 0.09$ for ^{L}HBD2/^{D}HBD2.

well to LF. The three native $^L\alpha$-defensins showed stronger LF binding than their corresponding D-enantiomers, although the differences measured by the RU values at 300 s of association were by and large within a factor of 2. Fitting of steady-state kinetic data is presented in Fig. 3, yielding the K_d values of the eight defensins for LF generally in line with the IC_{50} values determined by enzyme inhibition assays. For both L- and D-defensins, the order of LF-binding activity was: HNP1 ≈ HD5 > HNP4 ≫ HBD2. Importantly, the binding of D-defensins to LF decreased uniformly as compared with their corresponding L-forms. The -fold increase in K_d was ~5, 2, and 3 for ^{D}HNP1, ^{D}HNP4, and ^{D}HD5, respectively, consistent with the aforementioned changes in IC_{50}. ^{L}HBD2 and ^{D}HBD2 were excluded from the comparison, because their LF binding failed to approach saturation at the highest concentration used. Taken together, the LF inhibition and binding data suggest that D-defensins are weaker inhibitors of LF than their native forms, with the largest disparity seen for HNP1 and the smallest for HNP4.

D-Defensins Are Weaker Lectins Than L-Defensins—HNP1–3 and HD5, but not HNP4, HD6, and β-defensins, are known lectins that are capable of binding at high nanomolar affinities to HIV-1 gp120, a heavily glycosylated protein. To better understand lectin properties of enantiomeric defensins, we immobilized HIV_{BaL} gp120 (2830 RU for HNP1 and HD5, 3200 RU for HNP4) on a CM5 sensor chip and analyzed association and dissociation kinetics of various defensins at different concentrations. HNP1 and HD5 exhibited, from 250 nM to 8 μM, dose-dependent binding to gp120 (Fig. 4). No appreciable binding was observed with HBD2 at the highest concentration of 32 μM used (data not shown). ^{D}HNP1 and ^{D}HD5 were weaker than their corresponding L-forms. For direct comparison, the RU values at 300 s of all sensorgrams for HNP1 and HD5 were plotted *versus* defensin concentration. As shown in Fig. 4, the disparity between ^{L}HNP1 and ^{D}HNP1 in their ability to bind HIV gp120 varied from 10- to 5-fold as the defensin concentration increased from 250 nM to 8 μM. A similar disparity varying from 16- to 5-fold was found between ^{L}HD5 and ^{D}HD5 within the same concentration range. We did not try to fit the kinetic data to any mathematical model to obtain K_d values due to known mechanistic complexities associated with multivalent carbohydrate-binding and binding-induced self-oligomerization of HNP1 and HD5 on the surface of glycoproteins (56).

HNP4 showed greatly reduced ability to bind gp120 compared with HNP1 and HD5, consistent with our previous obser-

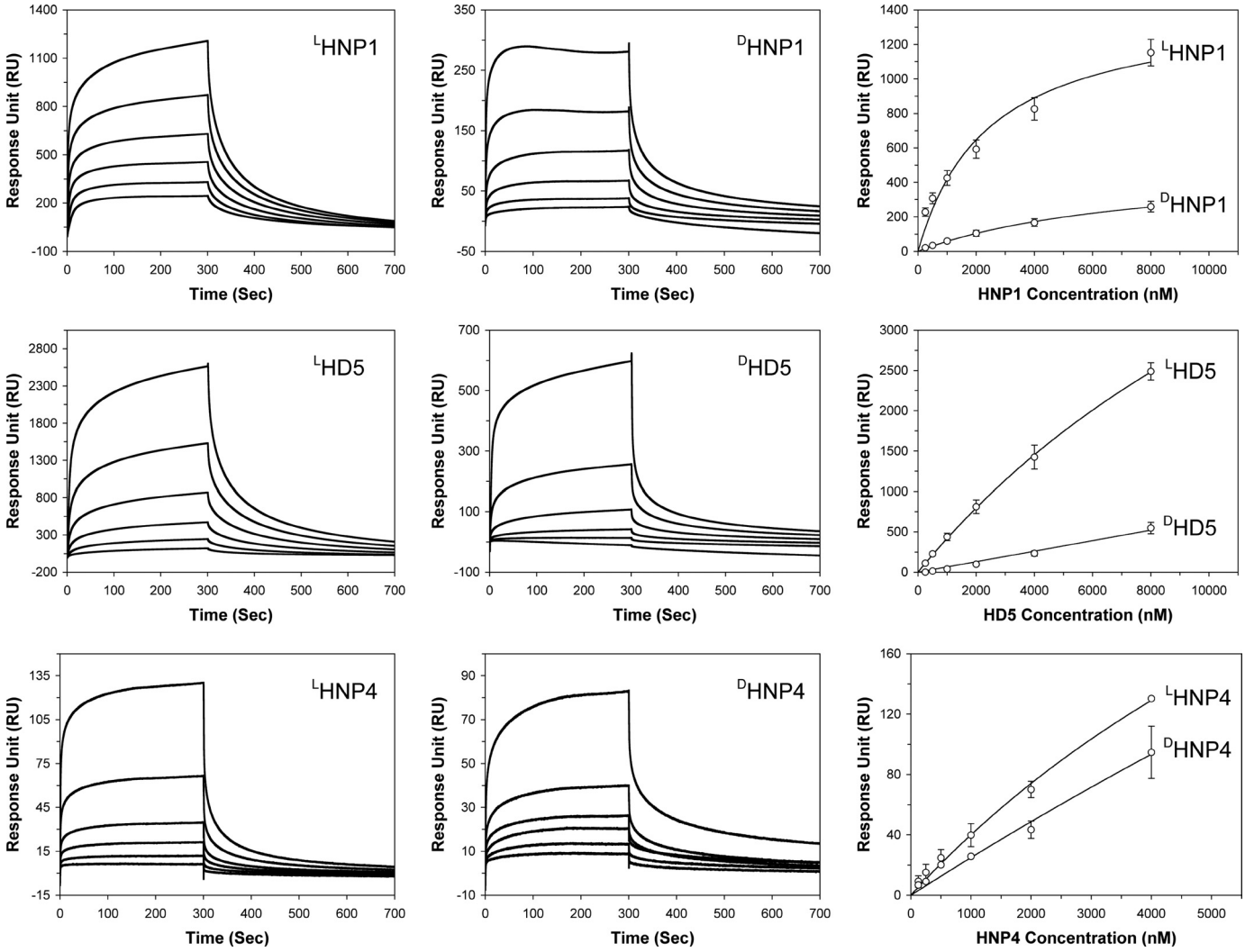

FIGURE 4. **Binding of enantiomeric defensins to HIV gp120.** *Left* and *middle columns*: representative sensorgrams of enantiomeric defensins at different concentrations (from 250 nM to 8 μM for HNP1 and HD5, and from 125 nM to 4 μM for HNP4). A sensor chip with 2830 RUs of gp120 was used for HNP1 and HD5 binding, and 3200 RUs of gp120 were immobilized for HNP4 measurements. *Right column*: RU values at 300 s of association from three independent SPR measurements were fitted to a one-site binding model ($Y = B_{max} \cdot X/[K_d + X]$) using GraphPad Prism version 4.0. The *p* values for statistical significance are: $p = 0.003$ for ^{L}HNP1/^{D}HNP1, $p = 0.022$ for ^{L}HD5/^{D}HD5, and $p = 0.024$ for ^{L}HNP4/^{D}HNP4.

vations (57). Further, unlike HNP1 and HD5, ^{D}HNP4 was only slightly weaker than ^{L}HNP4 in gp120 binding within the concentration range tested (125 nM to 4 μM). Despite a much-reduced capacity to bind gp120 compared with their native molecules, ^{D}HNP1 and ^{D}HD5 were still better lectins than ^{L}HNP4. Interestingly, when HNP4 concentration was increased to 8 μM and above, a sudden surge in reference cell binding ensued, resulting in irregularly shaped sensorgrams drifting into the negative RU region (data not shown). A similar artifact occurred with ^{D}HNP4 at 8 μM and above, making it impossible to compare ^{L}HNP4 and ^{D}HNP4 binding to gp120 at higher concentrations. The anomalous behavior of HNP4 at high concentrations may reflect distinct oligomerization properties of this defensin.

Bactericidal Activities of D-Defensins Are Both Strain-dependent and Peptide-dependent—Membrane permeabilization as a possible mechanism for bacterial killing by cationic antimicrobial peptides received early support from the studies that demonstrated a non-receptor mediated pathway, initially evidenced by the finding that some antimicrobial peptides consisting exclusively of all D-amino acids were equally active as their natural L-form counterparts (58). To investigate whether enantiomeric defensins kill bacteria equivalently, we quantified bactericidal activities of ^{L}HNP1/^{D}HNP1, ^{L}HNP4/^{D}HNP4, ^{L}HD5/^{D}HD5, and ^{L}HBD2/^{D}HBD2 against *E. coli* and *S. aureus* using a previously established assay protocol termed virtual colony count (49). Defensin dose-dependent survival of both strains are plotted in Fig. 5. As expected, the α-defensins, except for HNP4, killed the Gram-positive strain much more efficiently, whereas the β-defensin HBD2 exhibited strong bactericidal activity against the Gram-negative strain.

As anticipated, each of the four enantiomeric defensin pairs showed nearly identical killing activity against *E. coli*, consistent with the premise that induction of bacterial cell lysis by cationic antimicrobial peptides does not involve proteinaceous receptors on the cell membrane. Surprisingly and importantly, the validity of a unitary, membrane-only model was seriously undermined when we examined the killing of *S. aureus* by

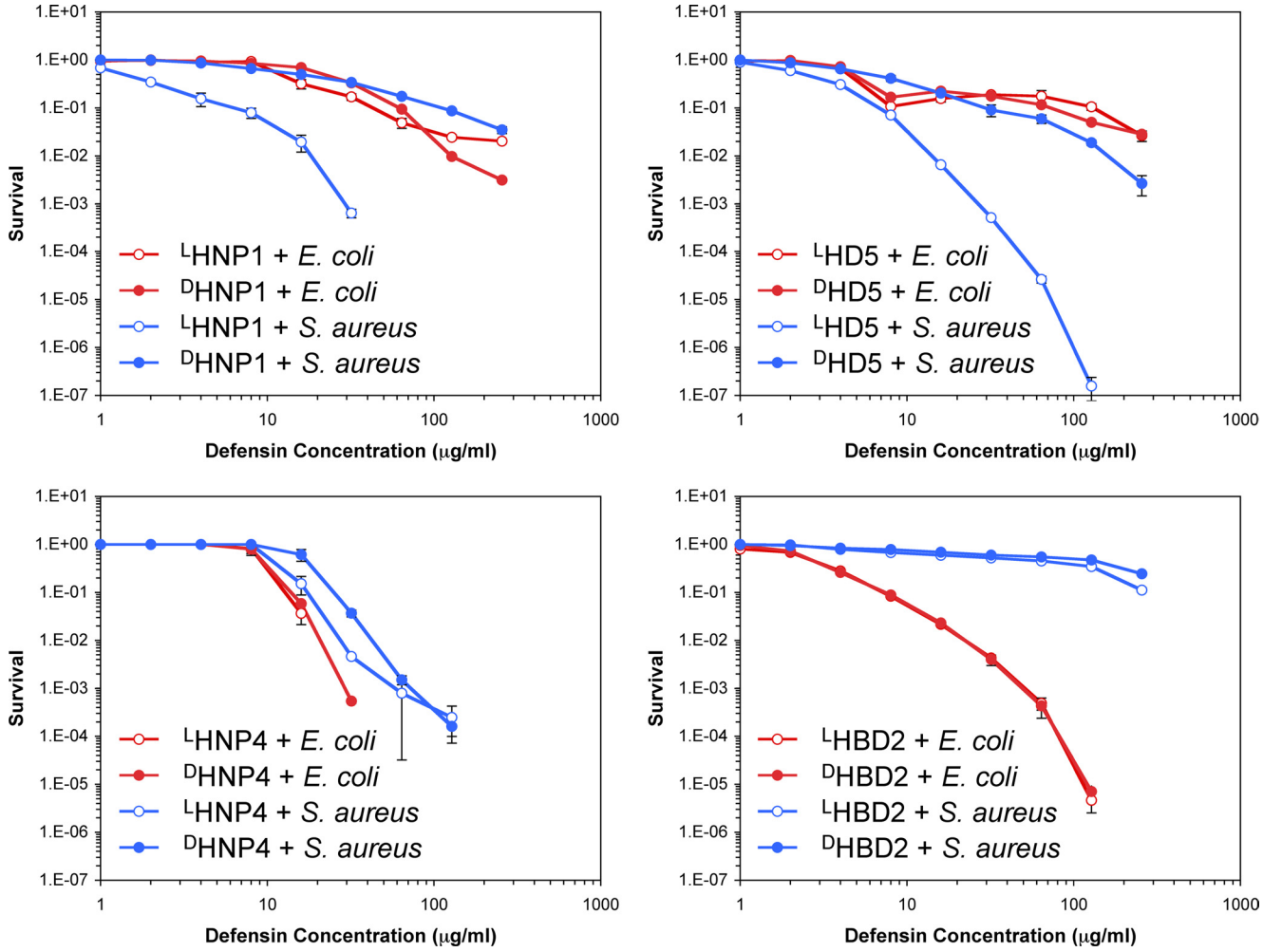

FIGURE 5. **Survival curves of *E. coli* ATCC 25922 (*red*) and *S. aureus* ATCC 29213 (*blue*) exposed to L- (*empty circles*) and D-defensin (*filled circles*).** Strains were exposed to the peptides at concentrations varying 2-fold from 1 to 256 μg/ml. Each *curve* is the mean of two (HNP1, HD5, and HBD2) or three (HNP4) separate experiments, where the *error bars* represent the ±S.D. of the measurements. Points scored as zero survival could not be plotted.

HNP1 and HD5. Here, ^{D}HNP1 and ^{D}HD5 displayed significantly reduced bactericidal activity compared with ^{L}HNP1 and ^{L}HD5, respectively. Upon L → D inversion of HNP1, the vLD_{50} value increased from 1.5 μg/ml to 16 μg/ml, while the vLD_{90} value increased by a factor of 19 (6 μg/ml to 115 μg/ml). At 64 μg/ml, ^{L}HNP1 quantitatively killed *S aureus*; bacterial growth could not be measured after the 12-h incubation time. In contrast, ^{D}HNP1 at the highest concentration of 256 μg/ml reduced *S. aureus* survival by <2 logs. Similar, but smaller differences were obtained with HD5. For HD5, the vLD_{50} value increased from 2.5 μg/ml for the L-form to 6.4 μg/ml for the D-form, whereas the vLD_{90} value increased only by a factor of 4.6 (from 7.3 μg/ml to 33 μg/ml).

Enantiomerization of HNP4 resulted in little change in its activity and selectivity toward both strains tested. This finding coincides with the earlier observation that inversion of HNP4 to its D-enantiomer exerted the least deleterious effect on HNP4 binding or inhibition of LF and gp120. HBD2 was extremely weak against *S. aureus*, and it was not possible to determine if its bactericidal activity against the Gram-positive strain was sensitive to enantiomerization.

It was recognized that target cell growth and metabolism greatly sensitized microbes to the killing of less cationic defensins such as HNP-1 and -2 and rabbit defensin NP-5 (as opposed to highly cationic defensins such as rabbit NP-1 and NP-2) (11, 59, 60). Consistent with these older observations, the addition of 1% TSB to the phosphate buffer during the initial 2-h incubation period in our vCC assay produced lower survival at a given concentration of HNP1 compared with that in the absence of TSB (Figs. 5 and 6). ^{L}HNP1 and ^{D}HNP1 showed much enhanced and nearly identical bactericidal activity against *E. coli* in the presence of 1% TSB. Providing nutrients that allowed bacterial growth enhanced the killing of *S. aureus* by both ^{L}HNP1 and ^{D}HNP1, without eliminating the much greater susceptibility of the Gram-positive strain to the L-enantiomer, as was also observed in the absence of TSB. The presence of 1% TSB made *E. coli* considerably more susceptible than *S. aureus* to HBD2. In their totality, the data related to chirality in Figs. 5 and 6 indicate that the mechanism whereby α-defensins HNP1 and HD5 kill *E. coli* is distinct from the mechanism that they use to kill *S. aureus*, because only the latter is chirality-dependent. The staphylococcal partner in this chiral interaction remains to be identified.

Other Human Defensins—We also tested HNP2, HNP3, HD6, HBD1, and HBD3 with respect to their inhibition of LF activity (Fig. 7*A*). HNP2 and HNP3 differ from HNP1 by one

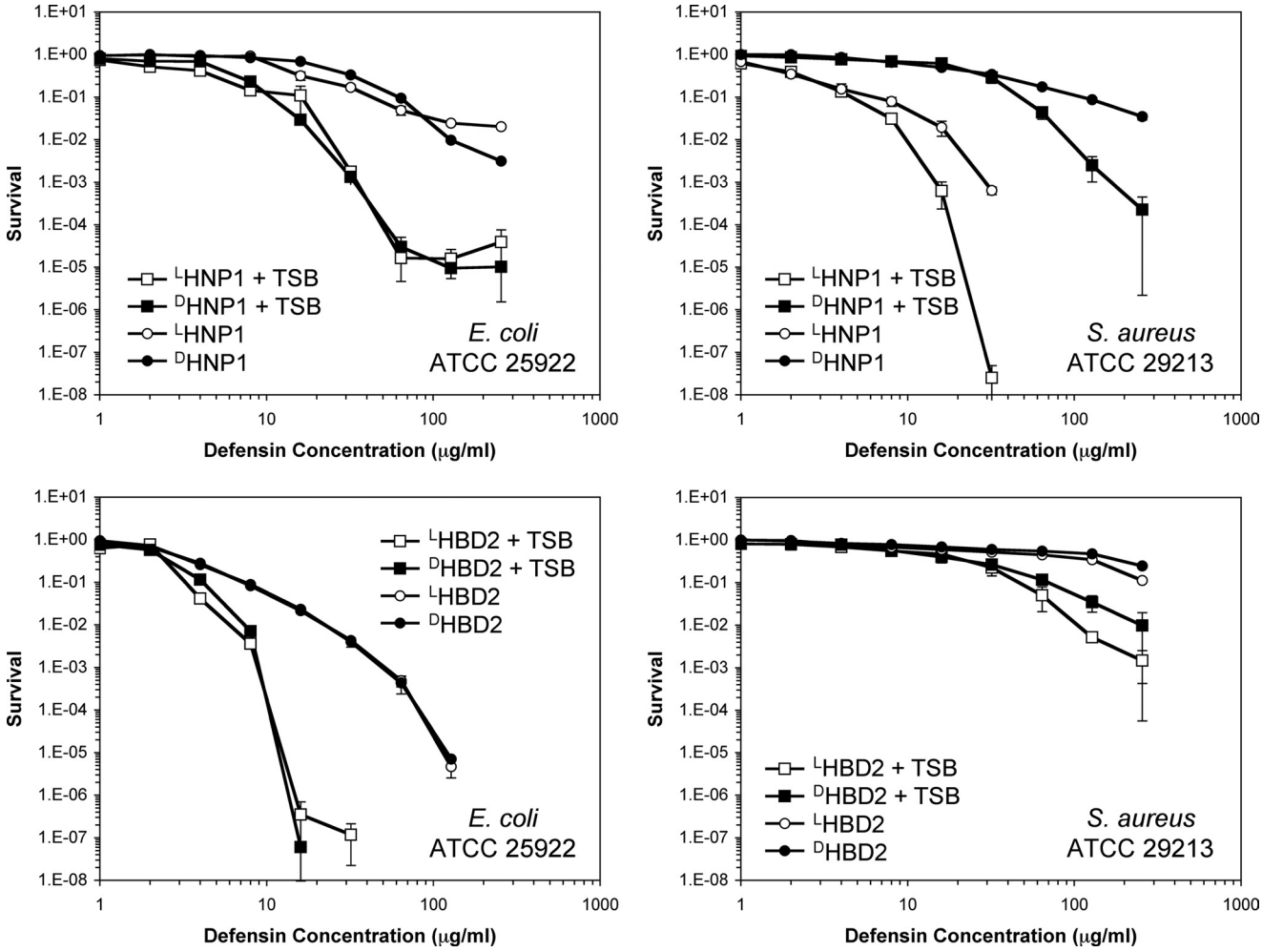

FIGURE 6. **Survival curves of *E. coli* ATCC 25922 and *S. aureus* ATCC 29213 exposed to L- (*empty symbols*) and D-defensin (*filled symbols*) in the presence (*squares*) and absence (*circles*) of 1% TSB.** Strains were exposed to the peptides at concentrations varying 2-fold from 1 to 256 μg/ml. Each *curve* is the mean of two separate experiments, where the *error bars* represent the ±S.D. of the measurements. Points scored as zero survival could not be plotted.

amino acid residue at the N terminus, and, as expected, had similar IC_{50} values to that of HNP1. HD6 was the weakest among the six α-defensins, with its maximal inhibitory activity leveling off at ~50% inhibition of LF. The reason that HD6 failed to progress beyond this plateau remains to be determined, but may be related to its ability to oligomerize differently from other human α-defensins (55). HBD1 had the highest IC_{50} value of 167 μM in the panel of nine native defensins tested. Notably, HBD3 is as active as HD5 against LF, and two orders of magnitude more potent than HBD2. These inhibitory activity data are in general agreement with the results obtained from SPR-based binding studies on immobilized LF and gp120 (Fig. 7*B*). The nine native defensins can be classified into three categories on the basis of their LF inhibition and gp120 binding activity: strong (HNP1, HNP2, HNP3, HD5 and HBD3), medium (HNP4), and weak (HBD1, HBD2 and HD6).

Defensin Tertiary Structure in Relation to LF Inhibition, HIV gp120 Binding, and Bacterial Killing—Kaufmann and colleagues reported that dithiothreitol-reduced HNP1 failed to inhibit LF (36). Reduction of the three disulfides followed by *S*-alkylation in retrocyclin-1 also dramatically reduced the ability of the θ-defensin to inhibit LF (38). To better understand the effect of disulfide bonding on LF inhibition, we characterized the unstructured forms of HNP1, HD5, and HBD3, in which all six Cys residues were simultaneously replaced by either Ala (in HNP1) or α-aminobutyric acid (in HD5 and HBD3). Dose-dependent LF inhibition by the three linearized defensins, designated as ^{linear}HNP1, ^{linear}HD5, and ^{linear}HBD3, is shown in Fig. 7*C*. For comparison, the inhibition curves of native HNP1, HD5, and HBD3 are also plotted in the same figure. For the two α-defensins, loss of their tertiary structure was clearly detrimental to LF inhibition. A reduction in LF inhibition by 110-fold, characterized by an increase in IC_{50} from 148 nM to 16.3 μM, was seen with HNP1, whereas the inhibitory activity of HD5 was weakened by 47-fold (an increase in IC_{50} from 194 nM to 9.2 μM). By contrast, loss of disulfide bonding in HBD3 had a much smaller effect on LF inhibition, as evidenced by a <4-fold increase in IC_{50} from 235 to 840 nM. The three unstructured defensins were also analyzed along with wild-type HNP1, HD5, and HBD3 with respect to their binding to LF, and, as shown in Fig. 8 (*top panel*), the SPR data fully agreed with the above findings. Further, disulfide bonding was also much less important for HBD3 than for HNP1 and HD5 in HIV gp120 binding (Fig. 8, *bottom panel*).

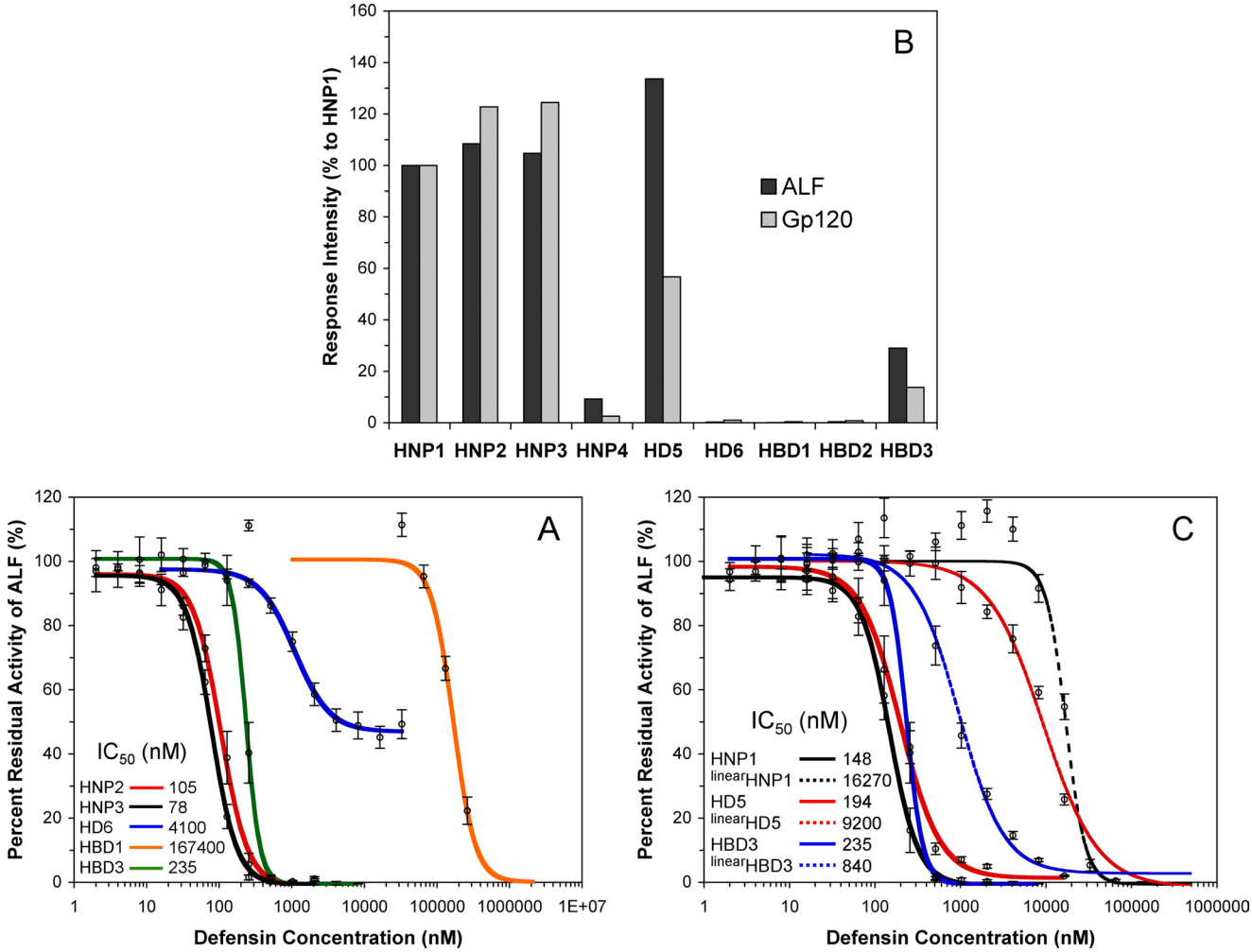

FIGURE 7. **Inhibition and binding of LF by other defensins.** *A*, inhibition of LF activity by different concentrations of HNP2 (*red*), HNP3 (*black*), HD6 (*blue*), HBD1 (*orange*), and HBD3 (*green*). *B*, percent RU, relative to HNP1, at 300 s of association of 100 nM defensin on 2500 RUs of immobilized LF or 2830 RUs of immobilized gp120. *C*, inhibition of LF activity by linearized defensins (*dotted lines*): ^{linear}HNP1 (*black*), ^{linear}HD5 (*red*), and ^{linear}HBD3 (*blue*). Each inhibition *curve* is the mean of three independent enzyme kinetic measurements. The *p* values for statistical significance are: $p = 0.0012$ for HNP1/^{linear}HNP1, $p = 0.0046$ for HD5/^{linear}HD5, and $p = 0.0076$ for HBD3/^{linear}HBD3.

Using virtual colony count, we have previously shown that ^{linear}HD5 was significantly less active than HD5 in killing *S. aureus*, but largely indistinguishable from HD5 in the killing of *E. coli* (61). We have extended the same observation to ^{linear}HNP1 and HNP1 under identical assay conditions. Shown in Fig. 9*A* are plots of *E. coli* and *S. aureus* survival *versus* defensin concentration. Both HNP1 and ^{linear}HNP1 had similarly weak killing activity against *E. coli*. By contrast, although HNP1 quantitatively killed *S. aureus* at 64 μg/ml, ^{linear}HNP1 was barely active at the same concentration. The survival of *S. aureus* was reduced by less than one log by ^{linear}HNP1 at its highest concentration of 256 μg/ml tested. Clearly, native α-defensin structure, while dispensable in the killing of *E. coli*, is required for efficient killing of *S. aureus*, reminiscent of ^{D}HNP1 and ^{D}HD5.

Due to an unusually high number of cationic charges, the bactericidal activity of HBD3 is generally insensitive to loss of or topological change in disulfide bonding (44, 62, 63). To extend our previous observation (44), we quantified dose-dependent killing of *E. coli* and *S. aureus* by HBD3, ^{linear}HBD3, and 10 disulfide analogs (each with a unique three-disulfide connectivity different from the native S–S pairing (Cys^1–Cys^5, Cys^2–Cys^4, and Cys^3–Cys^6). As shown in Fig. 9 (*B* and *C*), HBD3 and all its disulfide analogs, regardless of whether or not and how their disulfide bridges are paired, efficiently killed both strains of bacteria, with vLD_{90} values clustering around 6.6 ± 1.9 μg/ml for *E. coli* and 3.7 ± 1.0 μg/ml for *S. aureus*, and an identical average vLD_{50} value of 2.0 ± 0.5 μg/ml for both strains. At 25 μg/ml, complete killing of *E. coli* was achieved by all disulfide-bridged defensins, representing a reduction of the number of colonies by at least six orders of magnitude. By contrast, an average reduction of the number of colonies of *S. aureus* was approximately three orders of magnitude at the same defensin concentration.

DISCUSSION

Defensins are inherently effective multitaskers. How such small peptides have acquired functional versatility in innate and adaptive immunity is not well understood at the molecular level. The mechanism whereby HNP 1–3 killed *E. coli* was described in 1989 (11). The authors noted that, under conditions that supported bactericidal activity, HNP-1 sequentially

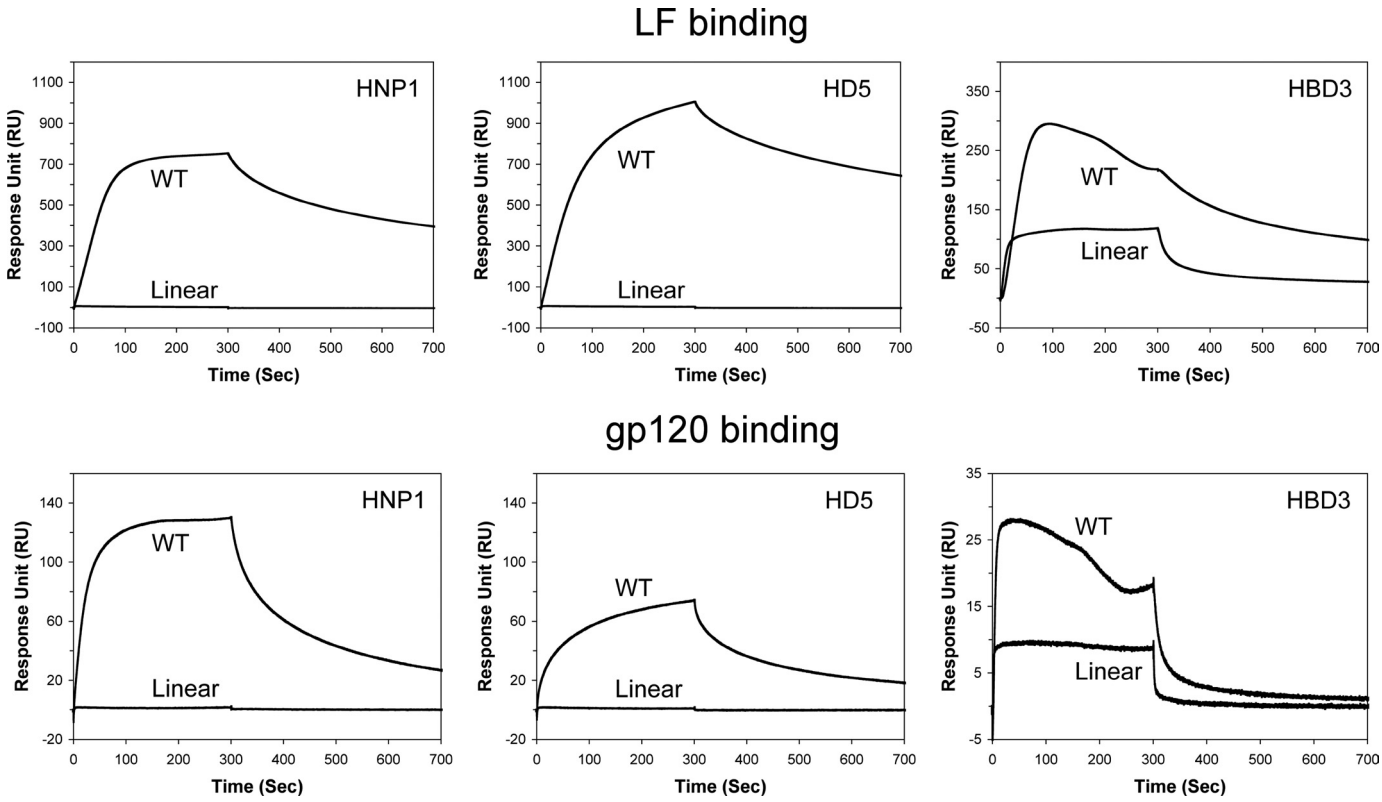

FIGURE 8. **Comparison of native HNP1, HD5, and HBD3 with their corresponding unstructured forms, each at 100 nM, in LF (*top panels*) and gp120 (*bottom panels*) binding.** Sensor chips with 2500 RUs of LF and 2830 RUs of gp120 were used for the SPR measurements.

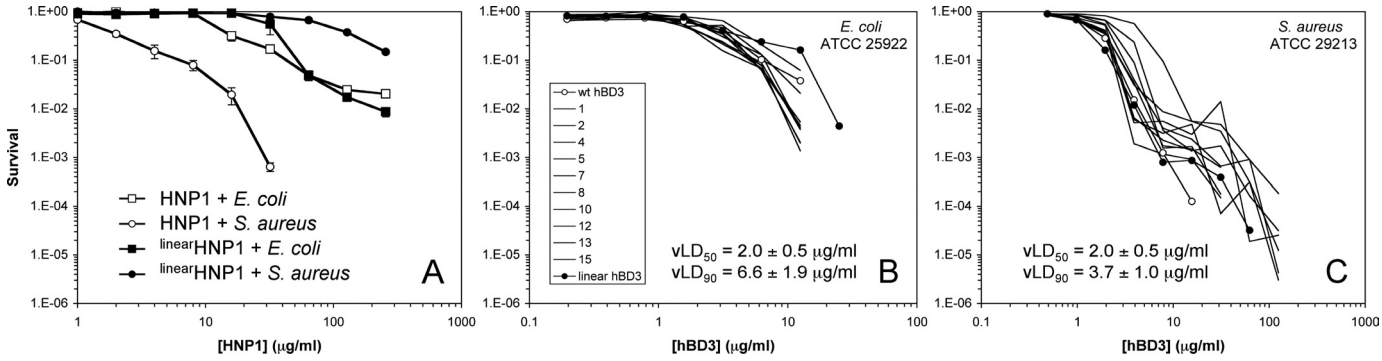

FIGURE 9. **Survival curves of *E. coli* ATCC 25922 and *S. aureus* ATCC 29213 exposed to HNP1 and ^{linear}HNP1 (*A*), and, to HBD3, ^{linear}HBD3 and 10 disulfide analogs of HBD3 (*B* and *C*).** Strains were exposed to the peptides at concentrations varying 2-fold from 1 to 256 μg/ml (HNP1 and ^{linear}HNP1), 0.195 to 50 μg/ml (HBD3 and *E. coli*), or 0.488 to 125 μg/ml (HBD3 and *S. aureus*). Each *curve* is the mean of two (HNP1 and ^{linear}HNP1) or three (HBD3 and analogs) separate experiments. Points scored as zero survival could not be plotted.

permeabilized the outer membrane and inner membrane of *E. coli* and that, coincident with these events, bacterial synthesis of DNA, RNA, and protein ceased and the colony count fell.

Merrifield and colleagues first used enantiomers to probe mechanisms of antimicrobial peptides (58) and reported in 1990 that the L- and D-enantiomers of three α-helical peptides (cecropin, magainin, or melittin) were equally active in polarizing planar lipid bilayers, killing Gram-positive and -negative strains of bacteria, and lysing erythrocytes. They suggested that chiral target cell molecules are not involved in the action of these antimicrobial peptides. We also noted functional equivalence of L- and D-enantiomers of protegrin-1, in studies performed with bacteria and *Candida albicans* (64–66). In contrast, when Tempst and colleagues studied enantiomers of apidaecins, proline- and arginine-rich antimicrobial peptides of insect origin that act preferentially on Gram-negative bacteria, the D-enantiomer proved to be much less potent (67, 68). They concluded that the peptides acted via a mechanism that included stereoselective elements but was completely devoid of any pore-forming activity. These earlier reports induced us to compare the functional properties of several paired D- and L-defensins. As discussed below, we gained some unexpected insights into the molecular basis for defensin function.

First, ^{D}HNP1 and ^{D}HD5 were significantly less active than their native L-forms in the killing of *S. aureus*, but the D- and L-enantiomers of HNP1 or HD5 were equally bactericidal against *E. coli*. This strain-dependent activity profile of D-defensins has unveiled a yet-to-be-recognized mechanistic com-

plexity of bacterial killing by defensins, likely arising from differences in the chemical composition and structure of the bacterial cell wall between *E. coli* and *S. aureus*.

For *S. aureus*, the cell wall consists primarily of a single but thick layer of peptidoglycan covered with (lipo)teichoic acid, whereas in *E. coli*, it is composed of a thin layer of peptidoglycan surrounded by a thin outer membrane whose outer leaflet is largely composed of lipopolysaccharide (69). Cationic antimicrobial peptides can associate with the negatively charged lipopolysaccharide or teichoic acid, an event thought to be important not only for antimicrobial selectivity but also for peptide uptake across the bacterial cell wall (70). It is plausible that an unidentified cellular component of *S. aureus*, possibly of chiral nature, preferably interacts with native defensins, thus contributing a great deal to bacterial killing. Consistent with this hypothesis, loss of the structure of HNP1 and HD5 dramatically reduced their bactericidal activity against *S. aureus* but not against *E. coli*. Our bactericidal data on HNP1 and HD5 as well as their linearized and D-enantiomeric analogs suggest that the membrane of *S. aureus* is not the sole lethal target for certain defensins and that an alternative mode of action exists in microbial killing.

Membrane-independent mechanisms have been proposed for bacterial killing by other classes of cationic antimicrobial peptides based on a poor correlation between their abilities to permeate model membranes and to kill bacteria (71). A poor correlation has also been established for the six human α-defensins between their membrane activity and bactericidal activity.[5] Hancock and colleagues argue that an alternative mode of action exists that likely involves internalization of cationic peptides and targeting of intracellular molecules (72, 73). The internal targeting hypothesis is supported by the observation that certain antimicrobial peptides interact with nuclear acids and interfere with protein synthesis but do not cause permanent membrane depolarization. Although it remains unclear how efficiently HNP1 and HD5 traverse the cytoplasmic membrane, the possibility of endocytic internalization cannot be ruled out. Alternatively, various effector molecules anchored on the cell wall surface may interact in the uptake process of certain defensins, thus facilitating or attenuating subsequent membrane permeabilization.

Nisin, an amphiphilic antibiotic peptide produced by various strains of *Lactococcus lactis*, is relatively weak in its ability to induce liposomal leakage but potently active in killing Gram-positive bacteria (74). Because the ability of nisin to induce liposomal leakage markedly increased by several orders of magnitude in the presence of Lipid II, a membrane-bound peptidoglycan precursor, it was suggested that nisin specifically binds to the pyrophosphate moiety of Lipid II for enhanced bacterial membrane permeabilization (75). More recently, nisin has been reported to displace Lipid II from the cell division site to block cell wall synthesis (76), a bacterial killing mechanism reminiscent of vancomycin (77). These findings raise an intriguing possibility, that is, HNP1 and HD5 may use some components of the bacterial cell wall or of the cytoplasmic membrane as docking molecules for enhanced membrane interaction and/or for inhibiting cell wall synthesis. Because HNP1 and HD5 are the strongest among the six human α-defensins in binding glycosylated proteins and peptidoglycans, the possibility merits further investigation. In this regard, lectin-like properties of HNP1 and HD5 may be functionally relevant to the killing of *S. aureus*.

A second surprising finding was the effective inhibition of LF by ^{D}HNP1 and ^{D}HD5 at high nanomolar concentrations. In nature, the L-amino acids are by far the predominant enantiomers (78). Whereas D-amino acids are commonly synthesized and incorporated into antibiotic peptides by prokaryotes, the animal kingdom restricts their appearance to post-translationally modified diastereomeric peptides in lower species, such as amphibians (79, 80). In humans, however, there exist no known D-amino acids. It is well established in the literature that the D-enantiomer of a native protein does not recognize the protein partners of the L-enantiomer or *vice versa* due to steric incompatibility. For example, a chemically synthesized D-HIV-1 protease does not hydrolyze natural substrates of the native viral protease but cleaves the D-enantiomer of a natural substrate as efficiently as L-HIV-1 protease cleaves the L-substrate (81). This chiral mode of molecular recognition is stringently maintained in interacting protein systems such as enzyme-substrate and enzyme-inhibitor. For these reasons, D-defensins were not expected to "specifically" interact with LF with high affinity. The fact that D-defensins were effective inhibitors of LF, as was the case with D-retrocyclins (38), suggests that defensin association with LF and many other proteins may be driven by forces that act in a nonspecific and non-directional fashion.

Defensins are small enough that both cationic and hydrophobic residues are solvent-exposed, a circumstance that makes the peptides unusually "sticky." It is plausible that these surface electrostatic and hydrophobic forces, in combination with a disulfide-stabilized molecular scaffold, enable multiple defensin molecules to bind a single target protein molecule. In fact, both HNP1 and HD5 have been shown to bind bacterial toxins and HIV gp120 at a high molar ratio (56, 82). Further, defensins can dimerize and potentially form higher order soluble aggregates in solution (6, 55). It has been demonstrated that binding of HNP1 or HD5 to gp120 or bacterial toxins promotes defensin self-aggregation (56, 82). Defensin oligomerization affords additional molecular complexity at the quaternary structural level, thereby contributing to enhanced structural diversity and functional versatility.

Finally, we observed that LF inhibition, gp120 binding, and *S. aureus* killing were strongly correlated among the various defensins studied. In general, the strongest inhibitors of LF were also the most effective bactericidal agents of *S. aureus* and often the best lectins. This is surprising given the different nature of the three defensin targets: a bacterial enzyme, a viral glycoprotein, and a bacterium. Does this correlation hint at a common molecular mechanism that allows defensins to intervene in so many diverse biological processes? Presently, we are exploring the possibility that events at the quaternary structural level, such as *in situ* oligomerization, may provide a common driving force that is ultimately responsible for modulating the

[5] P. Zeng, C. Xie, B. Ericksen, Z. Wu, X. Li, W.-Y. Lu, and W. Lu, unpublished results.

interaction of defensins with diverse targets and endowing them with so broad an array of functional properties.

Several conserved structural elements in α-defensins have been investigated, including a salt bridge, an invariant Gly residue, and disulfide bonding (83–87). However, these studies do not address the structural determinants that make some α-defensins considerably more potent than others in accomplishing a given task.

REFERENCES

1. Zasloff, M. (2002) *Nature* **415,** 389–395
2. Selsted, M. E., and Ouellette, A. J. (2005) *Nat. Immunol.* **6,** 551–557
3. Lehrer, R. I. (2004) *Nat. Rev. Microbiol.* **2,** 727–738
4. Ganz, T. (2003) *Nat. Rev. Immunol.* **3,** 710–720
5. Bevins, C. L. (2006) *Biochem. Soc. Trans.* **34,** 263–266
6. Pazgier, M., Hoover, D. M., Yang, D., Lu, W., and Lubkowski, J. (2006) *Cell Mol. Life Sci.* **63,** 1294–1313
7. Tang, Y. Q., Yuan, J., Osapay, G., Osapay, K., Tran, D., Miller, C. J., Ouellette, A. J., and Selsted, M. E. (1999) *Science* **286,** 498–502
8. Ganz, T., Selsted, M. E., Szklarek, D., Harwig, S. S., Daher, K., Bainton, D. F., and Lehrer, R. I. (1985) *J. Clin. Invest.* **76,** 1427–1435
9. Selsted, M. E., Harwig, S. S., Ganz, T., Schilling, J. W., and Lehrer, R. I. (1985) *J. Clin. Invest.* **76,** 1436–1439
10. Kagan, B. L., Selsted, M. E., Ganz, T., and Lehrer, R. I. (1990) *Proc. Natl. Acad. Sci. U.S.A.* **87,** 210–214
11. Lehrer, R. I., Barton, A., Daher, K. A., Harwig, S. S., Ganz, T., and Selsted, M. E. (1989) *J. Clin. Invest.* **84,** 553–561
12. Chang, T. L., Vargas, J., Jr., DelPortillo, A., and Klotman, M. E. (2005) *J. Clin. Invest.* **115,** 765–773
13. Sun, L., Finnegan, C. M., Kish-Catalone, T., Blumenthal, R., Garzino-Demo, P., La Terra Maggiore, G. M., Berrone, S., Kleinman, C., Wu, Z., Abdelwahab, S., Lu, W., and Garzino-Demo, A. (2005) *J. Virol.* **79,** 14318–14329
14. Quiñones-Mateu, M. E., Lederman, M. M., Feng, Z., Chakraborty, B., Weber, J., Rangel, H. R., Marotta, M. L., Mirza, M., Jiang, B., Kiser, P., Medvik, K., Sieg, S. F., and Weinberg, A. (2003) *AIDS* **17,** F39–F48
15. Mackewicz, C. E., Yuan, J., Tran, P., Diaz, L., Mack, E., Selsted, M. E., and Levy, J. A. (2003) *AIDS* **17,** F23–F32
16. Guo, C. J., Tan, N., Song, L., Douglas, S. D., and Ho, W. Z. (2004) *AIDS* **18,** 1217–1218
17. Gallo, S. A., Wang, W., Rawat, S. S., Jung, G., Waring, A. J., Cole, A. M., Lu, H., Yan, X., Daly, N. L., Craik, D. J., Jiang, S., Lehrer, R. I., and Blumenthal, R. (2006) *J. Biol. Chem.* **281,** 18787–18792
18. Furci, L., Sironi, F., Tolazzi, M., Vassena, L., and Lusso, P. (2007) *Blood* **109,** 2928–2935
19. Klotman, M. E., Rapista, A., Teleshova, N., Micsenyi, A., Jarvis, G. A., Lu, W., Porter, E., and Chang, T. L. (2008) *J. Immunol.* **180,** 6176–6185
20. Yang, D., Biragyn, A., Hoover, D. M., Lubkowski, J., and Oppenheim, J. J. (2004) *Annu Rev. Immunol.* **22,** 181–215
21. Rehaume, L. M., and Hancock, R. E. (2008) *Crit. Rev. Immunol.* **28,** 185–200
22. Funderburg, N., Lederman, M. M., Feng, Z., Drage, M. G., Jadlowsky, J., Harding, C. V., Weinberg, A., and Sieg, S. F. (2007) *Proc. Natl. Acad. Sci. U.S.A.* **104,** 18631–18635
23. Territo, M. C., Ganz, T., Selsted, M. E., and Lehrer, R. (1989) *J. Clin. Invest.* **84,** 2017–2020
24. Yang, D., Chen, Q., Chertov, O., and Oppenheim, J. J. (2000) *J. Leukoc. Biol.* **68,** 9–14
25. Yang, D., Chertov, O., Bykovskaia, S. N., Chen, Q., Buffo, M. J., Shogan, J., Anderson, M., Schröder, J. M., Wang, J. M., Howard, O. M., and Oppenheim, J. J. (1999) *Science* **286,** 525–528
26. van Wetering, S., Mannesse-Lazeroms, S. P., van Sterkenburg, M. A., and Hiemstra, P. S. (2002) *Inflamm. Res.* **51,** 8–15
27. Shi, J., Aono, S., Lu, W., Ouellette, A. J., Hu, X., Ji, Y., Wang, L., Lenz, S., van Ginkel, F. W., Liles, M., Dykstra, C., Morrison, E. E., and Elson, C. O. (2007) *J. Immunol.* **179,** 1245–1253
28. van den Berg, R. H., Faber-Krol, M. C., van Wetering, S., Hiemstra, P. S., and Daha, M. R. (1998) *Blood* **92,** 3898–3903
29. Panyutich, A. V., Szold, O., Poon, P. H., Tseng, Y., and Ganz, T. (1994) *FEBS Lett.* **356,** 169–173
30. Sørensen, O. E., Cowland, J. B., Theilgaard-Mönch, K., Liu, L., Ganz, T., and Borregaard, N. (2003) *J. Immunol.* **170,** 5583–5589
31. Aarbiou, J., Ertmann, M., van Wetering, S., van Noort, P., Rook, D., Rabe, K. F., Litvinov, S. V., van Krieken, J. H., de Boer, W. I., and Hiemstra, P. S. (2002) *J. Leukoc. Biol.* **72,** 167–174
32. Candille, S. I., Kaelin, C. B., Cattanach, B. M., Yu, B., Thompson, D. A., Nix, M. A., Kerns, J. A., Schmutz, S. M., Millhauser, G. L., and Barsh, G. S. (2007) *Science* **318,** 1418–1423
33. Lehrer, R. I. (2007) *Curr. Opin Hematol.* **14,** 16–21
34. Moayeri, M., and Leppla, S. H. (2004) *Curr. Opin. Microbiol.* **7,** 19–24
35. Collier, R. J., and Young, J. A. (2003) *Annu. Rev. Cell Dev. Biol.* **19,** 45–70
36. Kim, C., Gajendran, N., Mittrücker, H. W., Weiwad, M., Song, Y. H., Hurwitz, R., Wilmanns, M., Fischer, G., and Kaufmann, S. H. (2005) *Proc. Natl. Acad. Sci. U.S.A.* **102,** 4830–4835
37. Mayer-Scholl, A., Hurwitz, R., Brinkmann, V., Schmid, M., Jungblut, P., Weinrauch, Y., and Zychlinsky, A. (2005) *PLoS Pathog.* **1,** e23
38. Wang, W., Mulakala, C., Ward, S. C., Jung, G., Luong, H., Pham, D., Waring, A. J., Kaznessis, Y., Lu, W., Bradley, K. A., and Lehrer, R. I. (2006) *J. Biol. Chem.* **281,** 32755–32764
39. Leikina, E., Delanoe-Ayari, H., Melikov, K., Cho, M. S., Chen, A., Waring, A. J., Wang, W., Xie, Y., Loo, J. A., Lehrer, R. I., and Chernomordik, L. V. (2005) *Nat. Immunol.* **6,** 995–1001
40. Münk, C., Wei, G., Yang, O. O., Waring, A. J., Wang, W., Hong, T., Lehrer, R. I., Landau, N. R., and Cole, A. M. (2003) *AIDS Res. Hum. Retroviruses* **19,** 875–881
41. Wang, W., Owen, S. M., Rudolph, D. L., Cole, A. M., Hong, T., Waring, A. J., Lal, R. B., and Lehrer, R. I. (2004) *J. Immunol.* **173,** 515–520
42. Wang, W., Cole, A. M., Hong, T., Waring, A. J., and Lehrer, R. I. (2003) *J. Immunol.* **170,** 4708–4716
43. Wu, Z., Ericksen, B., Tucker, K., Lubkowski, J., and Lu, W. (2004) *J. Pept. Res.* **64,** 118–125
44. Wu, Z., Hoover, D. M., Yang, D., Boulègue, C., Santamaria, F., Oppenheim, J. J., Lubkowski, J., and Lu, W. (2003) *Proc. Natl. Acad. Sci. U.S.A.* **100,** 8880–8885
45. Wu, Z., Powell, R., and Lu, W. (2003) *J. Am. Chem. Soc.* **125,** 2402–2403
46. Schnölzer, M., Alewood, P., Jones, A., Alewood, D., and Kent, S. B. (1992) *Int. J. Pept. Protein Res.* **40,** 180–193
47. Pace, C. N., Vajdos, F., Fee, L., Grimsley, G., and Gray, T. (1995) *Protein Sci.* **4,** 2411–2423
48. Min, D. H., Tang, W. J., and Mrksich, M. (2004) *Nat. Biotechnol.* **22,** 717–723
49. Ericksen, B., Wu, Z., Lu, W., and Lehrer, R. I. (2005) *Antimicrob. Agents Chemother.* **49,** 269–275
50. Otwinowski, Z., and Minor, W. (1997) *Methods Enzymol.* **276,** 307–326
51. Storoni, L. C., McCoy, A. J., and Read, R. J. (2004) *Acta Crystallogr. D Biol. Crystallogr.* **60,** 432–438
52. Hill, C. P., Yee, J., Selsted, M. E., and Eisenberg, D. (1991) *Science* **251,** 1481–1485
53. Murshudov, G. N., Vagin, A. A., and Dodson, E. J. (1997) *Acta Crystallogr. D Biol. Crystallogr.* **53,** 240–255
54. Emsley, P., and Cowtan, K. (2004) *Acta Crystallogr. D Biol. Crystallogr.* **60,** 2126–2132
55. Szyk, A., Wu, Z., Tucker, K., Yang, D., Lu, W., and Lubkowski, J. (2006) *Protein Sci.* **15,** 2749–2760
56. Lehrer, R. I., Jung, G., Ruchala, P., Andre, S., Gabius, H. J., and Lu, W. (2009) *J. Immunol.* **183,** 480–490
57. Wu, Z., Cocchi, F., Gentles, D., Ericksen, B., Lubkowski, J., Devico, A., Lehrer, R. I., and Lu, W. (2005) *FEBS Lett.* **579,** 162–166
58. Wade, D., Boman, A., Wåhlin, B., Drain, C. M., Andreu, D., Boman, H. G., and Merrifield, R. B. (1990) *Proc. Natl. Acad. Sci. U.S.A.* **87,** 4761–4765
59. Lehrer, R. I., Ganz, T., Szklarek, D., and Selsted, M. E. (1988) *J. Clin. Invest.* **81,** 1829–1835
60. Ganz, T., Selsted, M. E., and Lehrer, R. I. (1990) *Eur. J. Haematol.* **44,** 1–8
61. de Leeuw, E., Burks, S. R., Li, X., Kao, J. P., and Lu, W. (2007) *FEBS Lett.*

581, 515–520
62. Taylor, K., Clarke, D. J., McCullough, B., Chin, W., Seo, E., Yang, D., Oppenheim, J., Uhrin, D., Govan, J. R., Campopiano, D. J., MacMillan, D., Barran, P., and Dorin, J. R. (2008) *J. Biol. Chem.* **283,** 6631–6639
63. Klüver, E., Schulz-Maronde, S., Scheid, S., Meyer, B., Forssmann, W. G., and Adermann, K. (2005) *Biochemistry* **44,** 9804–9816
64. Kokryakov, V. N., Harwig, S. S., Panyutich, E. A., Shevchenko, A. A., Aleshina, G. M., Shamova, O. V., Korneva, H. A., and Lehrer, R. I. (1993) *FEBS Lett.* **327,** 231–236
65. Cho, Y., Turner, J. S., Dinh, N. N., and Lehrer, R. I. (1998) *Infect. Immun.* **66,** 2486–2493
66. Miyasaki, K. T., Iofel, R., Oren, A., Huynh, T., and Lehrer, R. I. (1998) *J. Periodontal Res.* **33,** 91–98
67. Casteels, P., and Tempst, P. (1994) *Biochem. Biophys. Res. Commun.* **199,** 339–345
68. Castle, M., Nazarian, A., Yi, S. S., and Tempst, P. (1999) *J. Biol. Chem.* **274,** 32555–32564
69. Brock, T. D., and Madigan, M. T. (1991) *Biology of Microorganisms*, Sixth Ed., pp. 54–62, Prentice-Hall, Englewood Cliffs, NJ
70. Hancock, R. E. (1997) *Lancet* **349,** 418–422
71. Brogden, K. A. (2005) *Nat. Rev. Microbiol.* **3,** 238–250
72. Wu, M., Maier, E., Benz, R., and Hancock, R. E. (1999) *Biochemistry* **38,** 7235–7242
73. Hancock, R. E., and Rozek, A. (2002) *FEMS Microbiol. Lett.* **206,** 143–149
74. Breukink, E., Wiedemann, I., van Kraaij, C., Kuipers, O. P., Sahl, H., and de Kruijff, B. (1999) *Science* **286,** 2361–2364
75. Hsu, S. T., Breukink, E., Tischenko, E., Lutters, M. A., de Kruijff, B., Kaptein, R., Bonvin, A. M., and van Nuland, N. A. (2004) *Nat. Struct. Mol. Biol.* **11,** 963–967
76. Hasper, H. E., Kramer, N. E., Smith, J. L., Hillman, J. D., Zachariah, C., Kuipers, O. P., de Kruijff, B., and Breukink, E. (2006) *Science* **313,** 1636–1637
77. Breukink, E., and de Kruijff, B. (2006) *Nat. Rev. Drug Discov.* **5,** 321–332
78. Kreil, G. (1997) *Annu. Rev. Biochem.* **66,** 337–345
79. Heck, S. D., Siok, C. J., Krapcho, K. J., Kelbaugh, P. R., Thadeio, P. F., Welch, M. J., Williams, R. D., Ganong, A. H., Kelly, M. E., Lanzetti, A. J., *et al*. (1994) *Science* **266,** 1065–1068
80. Kreil, G. (1994) *Science* **266,** 996–997
81. Milton, R. C., Milton, S. C., and Kent, S. B. (1992) *Science* **256,** 1445–1448
82. Lehrer, R. I., Jung, G., Ruchala, P., Wang, W., Micewicz, E. D., Waring, A. J., Gillespie, E. J., Bradley, K. A., Ratner, A. J., Rest, R. F., and Lu, W. (2009) *Infect. Immun.* **77,** 4028–4040
83. Wu, Z., Li, X., de Leeuw, E., Ericksen, B., and Lu, W. (2005) *J. Biol. Chem.* **280,** 43039–43047
84. Xie, C., Prahl, A., Ericksen, B., Wu, Z., Zeng, P., Li, X., Lu, W. Y., Lubkowski, J., and Lu, W. (2005) *J. Biol. Chem.* **280,** 32921–32929
85. Rajabi, M., de Leeuw, E., Pazgier, M., Li, J., Lubkowski, J., and Lu, W. (2008) *J. Biol. Chem.* **283,** 21509–21518
86. Maemoto, A., Qu, X., Rosengren, K. J., Tanabe, H., Henschen-Edman, A., Craik, D. J., and Ouellette, A. J. (2004) *J. Biol. Chem.* **279,** 44188–44196
87. Rosengren, K. J., Daly, N. L., Fornander, L. M., Jönsson, L. M., Shirafuji, Y., Qu, X., Vogel, H. J., Ouellette, A. J., and Craik, D. J. (2006) *J. Biol. Chem.* **281,** 28068–28078